ELSEVIER

Surface Science 490 (2001) 29–42

SURFACE SCIENCE

www.elsevier.com/locate/susc

Adatom interlayer diffusion on Pt(1 1 1): an embedded atom method study

G. Leonardelli, E. Lundgren [1], M. Schmid *

Institut für Allgemeine Physik, TU Wien, Wiedner Hauptstrasse 8-10, A-1040 Wien, Austria

Received 29 July 2000; accepted for publication 29 May 2001

Abstract

We use embedded atom method potentials to calculate the Schwoebel barriers for a large number of hopping and exchange processes of Pt and Ni adatoms descending steps of the Pt(1 1 1) surface. The barriers we find for hopping processes are too high to play any role in homo- and heteroepitaxy, but we find very low and even negative Schwoebel barriers for exchange processes at concave corners and kinks. On straight steps we find the process taking place on B-steps rather than on A-steps, with very similar Schwoebel barriers for Ni and Pt adatoms. We also find a strong dependence of the Schwoebel barrier on the lateral relaxation of step edges as caused by surface stress. For vicinal surfaces with high step density this effect causes an increase of the Schwoebel barrier if the width of the (1 1 1)-terraces is reduced. Due to the same effect, the barriers should be different for the small cell sizes of today's ab initio calculations as compared to larger terraces.

Keywords: Construction and use of effective interatomic interactions; Semi-empirical models and model calculations; Diffusion and migration; Growth; Surface diffusion; Surface stress; Nickel; Platinum

1. Introduction

Recently, a large number of investigations [1–13] have been devoted to investigate the details on how an atom diffuses across a step-edge from one terrace of a substrate crystal or thin film to a lower terrace. If an atom may cross a step without a significant difference in activation energy from that of the self-diffusion of the atom on the terrace E_D, smooth layer-by-layer growth (two-dimensional (2D) growth) is expected, while if the barrier is much larger than E_D and cannot be easily overcome by the thermal energy, three-dimensional (3D) growth is likely to prevail. In crystal growth, controlling, and thus understanding the growth mode is therefore closely connected to the understanding of the processes governing atomic diffusion across steps.

In general, an adatom approaching a descending step may cross the step by two different processes (see Fig. 1a), (i) by hopping over the step or (ii) the atom sinks into the surface behind a step edge atom, which is pushed onto the lower terrace (exchange process or concerted substitution). The

* Corresponding author. Tel.: +43-1-58801-13452; fax: +43-1-58801-13499.

E-mail address: schmid@iap.tuwien.ac.at (M. Schmid).

[1] Present address: Department of Synchrotron Radiation Research, Institute of Physics, University of Lund, Box 118, S-22100 Lund, Sweden.

0039-6028/01/$ - see front matter
PII: S0039-6028(01)01212-2

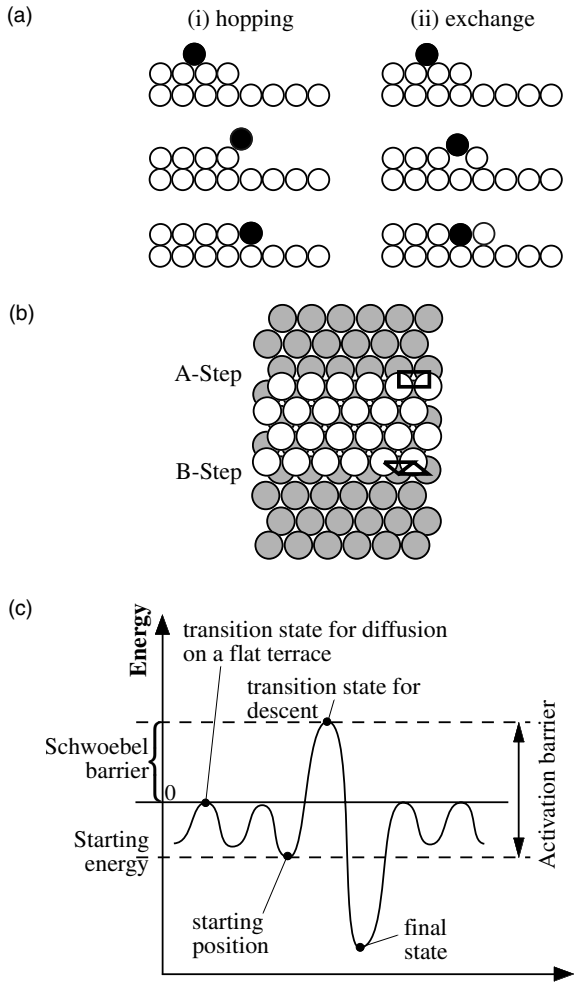

Fig. 1. (a) Schematic side view of adatom descent at a step. (b) Top-view of the fcc(1 1 1) surface illustrating A- and B-steps. (c) Energy along a diffusion path to illustrate the meaning of the Schwoebel barrier (see text for explanation).

energy activation barriers for these processes will determine whether interlayer mass transport is possible and which of the two will be the preferred process. In addition, on fcc(1 1 1) surfaces, as in the present paper, two different kinds of straight steps exist (see Fig. 1b), the so-called A- and B-steps, with {1 0 0} and {1 1 1} microfacets, respectively. The different geometries for the two steps, as may be seen in Fig. 1b, is known to influence the energy activation barrier for an atom diffusing across the step [1].

In addition to the influence of A- and B-steps on the interlayer diffusion, previous investigations have found indications for changes of the energy activation barriers at kinks and corners at the step edges. Simulations based on embedded atom method (EAM) [5] and effective medium theory (EMT) [6], have predicted low barriers for exchange processes at kinks. Such a scenario has been used to explain the phenomenon of the re-entrant layer by layer growth observed for Pt/Pt(1 1 1) [14, 15]. At high temperatures the growth is 2D. At intermediate temperatures, the growth becomes 3D, but at still lower temperatures it reverts back to 2D. The fact that small and irregular islands are observed at low temperature [14] supports the importance of kinks and corners for the growth mode. However, the effect of the size of the islands on the interlayer transport might also induce changes in the reflection-barrier at the step-edge for the adatom approaching the descending step [7,15]. Very recently, an STM investigation of Pt/Pt(1 1 1) [16] showed that the coarsening of the Pt adlayers was different at low and high Pt coverages, which was explained by the higher kink density at the steps at lower Pt coverages, lowering the effective activation barrier.

Studies on the atomic scale of the elementary steps in interlayer diffusion have so far displayed no homogeneous results concerning the preferred interlayer diffusion process or site, although the number of investigations is rather low. In the case of Al/Al(1 1 1) [12,13], ab initio calculations found a preference for interlayer transport via an exchange process, but a low energy barrier difference between this process occurring at an A- or a B-step (0.08 and 0.06 eV, respectively). These findings have yet to be confirmed experimentally. For Ag/Ag(1 1 1) energy activation barriers across the steps have been experimentally found to be large [17], explaining the rough appearance of the growth [18,19]. Field ion microscopy (FIM) shows that step descent of Ir on Ir(1 1 1) is easier at a B- than at an A-step [7]. Turning to previous investigations of heteroepitaxial growth on fcc(1 1 1) surfaces, two studies using FIM showed that W and Re atoms on Ir(1 1 1) diffuse over A-steps and undergo exchange at B-steps [7,8], and a recent STM study of Co on Pt(1 1 1) [20] suggests ex-

change processes only at the concave corners and kinks of both A- and B-steps.

For homoepitaxial growth of Pt on Pt(1 1 1), recent FIM investigations [7] found a lowest barrier for diffusion across a step of 0.36 eV but no details about the process were determined. This finding is in rough agreement with recent ab initio local density approximation (LDA) calculations resulting in a barrier of 0.31 eV for descent at the A-step [2]. The barrier heights calculated for an exchange process at the B-step and hopping over the A- and B-steps were found to be significantly larger (0.64, 0.53 and 0.80 eV, respectively). The fact that the exchange barrier for A-steps is close to the activation barrier for self-diffusion on the terrace ($E_D = 0.25$–0.29 eV, according to Refs. [2–4,10,11]), indicates that Pt on Pt(1 1 1) should grow 2D. Without contamination, 2D growth was indeed found experimentally [21] for low coverages. At these conditions, the steps are almost exclusively B-steps, however.

In this paper we calculate the energy barriers for descent of adatoms on the Pt(1 1 1) surface at A- and B-steps, and at many other sites at or next to kinks and corners. Our calculations are based on semiempirical EAM potentials. While not reaching the accuracy of ab initio studies, these potentials allow to use much larger cells. This is especially important as our results demonstrate a significant influence of the terrace size on the energy barriers calculated. Therefore, cell sizes between a few hundred and several thousand atoms are necessary for reliable calculations. The results for diffusion of two types of adatoms, Pt and Ni, show similar trends. We therefore argue that our calculations also support previous STM studies [20] of the initial growth of Co on Pt(1 1 1) with artificially created vacancy islands, where it was shown that Co adatoms coming from the upper terrace are favourably embedded behind corners and kinks.

2. Calculation method

As mentioned, to handle the large cell sizes necessary, we use semiempirical potentials, and among these we choose the EAM potentials adapted by Ritz et al. for the PtNi system [22]. These potentials have already been used successfully for surface studies of PtNi alloys [22,23]. As these potentials were developed with special care for a good description of bonding between Pt and Ni and the surface properties of their alloys, we can use them to study both Ni and Pt adatoms on Pt(1 1 1), allowing to determine the influence of the kind of adatom on the phenomena observed. The results for Pt and Ni will be shown to be rather similar, with both types of adatoms showing the same trends. We therefore believe that these trends will be also valid for Co, which has been used for the recent experiments of Lundgren et al. [20]. The similarity of Ni and Co is also supported by the almost identical surface properties of PtNi and PtCo alloys [24–31]. (It should be noted here that the standard procedure to develop EAM potentials is not directly applicable to Co, since its stable crystallographic structure below $\approx$450°C is hcp, not fcc.)

Methfessel et al. [32] has discussed in detail the dependence of the cohesive energy on the coordination number. In contrast to EAM-type potentials, where the energy smoothly approaches that of the free atom with decreasing coordination, it was shown that the energy as a function of coordination number actually behaves differently. The potentials we used have been tested in segregation calculations for coordination numbers higher than six [23] and proved sufficiently accurate, some extrapolation to lower coordination numbers should be possible. At the lowest coordination numbers (2 or 3) as they occur in hopping processes this must be considered problematic. This problem also affects surface self-diffusion on the fcc(1 1 1) surface, where the transition state is the twofold coordinated bridge position of the adatom between hcp and fcc hollow site.

To find the transition state of a process we let the system relax, and then forced one atom to move into a given direction in small steps. After each step the system was relaxed again, where the atom moved was constrained to the plane perpendicular to the direction of movement. In other words, we fixed one of the $3N$ degrees of freedom (of N atoms) and found the energy minimum for the remaining $3N-1$ degrees of freedom. The transition path then was sampled along the fixed

degree of freedom, and the point of maximum energy along this path taken as transition state. This procedure ensures that the forces in the transition state are zero. The atom we chose to move was the adatom in case of hopping processes, or the substrate atom exchanged in the exchange processes. Some care had to be taken with the choice of the direction of movement to avoid jumps in energy when the atom configuration suddenly changed to a more stable position. We made sure that the maximum of energy was flat and did not show a cusp. Typically there were about 10 energy samples within 1 meV from the maximum. The calculations have been done with the artwork program by Stoltze [33], which has been adapted in our group for the EAM-potentials [22] used. As an additional test, some processes have been re-calculated using the nudged elastic band method [34], yielding the same results.

To compare the probability of different diffusion processes to happen, it is not enough to compare the activation barriers. One must also take into account that the starting points for concurring processes are different and therefore usually have different adsorption energies. These different energies influence the probability of an adatom to occupy different positions and thereby change the probabilities that processes starting there can occur. A quantity taking this into account is the Ehrlich–Schwoebel barrier [35,36] (for short "Schwoebel barrier"), which is defined as the difference in energies between the transition state of step descent and that of diffusion over a flat terrace. To calculate the Schwoebel barrier of a process, one therefore not only needs to know the activation barrier, but also the activation barrier of diffusion over a perfect flat terrace, as well as the difference in adsorption energy of the adatom resting on the flat terrace and of the adatom in the starting position of the process in question (see Fig. 1c). The adsorption energy was calculated by moving the adatom from the surface to a distance beyond the cut-off of the potentials with full relaxation of all atoms performed before and after removing the adatom.

As mentioned, to calculate the Schwoebel barrier, we have to determine the barrier for self-diffusion of a Pt adatom on a Pt(1 1 1) surface. This turns out to be problematic, however. In our calculations in the transition state the Pt adatom does not sit in a bridge position, but rather sinks deeper into the surface, changing the bridge site to a metastable 4-fold hollow position. This leads to a shift of the transition state from the bridge position to a position between the fcc hollow site and the 4-fold hollow site, lowering the energy barrier to 46 meV and thereby raising the Schwoebel barriers given in this paper for Pt adatoms. For the Ni adatom no such metastable position was found, the activation barrier for self-diffusion was determined as 178 meV with the bridge position as the transition state. This is both an effect of the higher sensitivity a Pt atom has to coordination numbers, than the Ni adatom has [23], and an effect of the different sizes of the adatoms. A smaller adatom like Ni can not be near enough to four surface atoms to be 4-fold coordinated in the bridge site, whereas the larger Pt adatom can. Furthermore, on Pt(1 1 1) the smaller Ni adatom will sink into the surface more deeply than the Pt adatom and therefore see a higher corrugation of the potential energy surface. We therefore consider a higher diffusion barrier for Ni than that for Pt reasonable. The absolute numbers for the Pt adatom diffusion barriers calculated here are much too low (0.046 eV compared to 0.25 eV for FIM measurements [4] or 0.26 eV for STM experiments [11]), however. As mentioned previously, we attribute this to the low coordination in the transition state of self-diffusion not adequately described by the potentials used. As the diffusion barrier for self-diffusion enters the Schwoebel barriers only as a fixed offset, the trends and differences between different Schwoebel barriers will remain unaffected, whereas the absolute numbers calculated will be too high.

To calculate diffusion processes on straight steps, we set up vicinal surfaces. For the A-step we chose the (4,3,3) surface, and for the B-step the (4,4,3) surface. Both have a terrace width of seven atoms. We took six layers with the atoms of the lowest two fixed in bulk positions, and a periodicity of eight atoms along the step edge.

To investigate the influence of in-plane surface stress on the activation barriers we set up a slab with a periodicity of 8×8 atoms (six layers thick, the two bottom layers fixed). On this slab a four

atom wide stripe shaped island was placed as shown in Fig. 1b. The atoms on one step edge were moved in-plane perpendicular to the step to increase or decrease the stress on the opposite step. This row of atoms, as well as the row directly underneath was then fixed in position, and the calculation for step descent at the free step was performed as before. As the crystal gets sheared by this procedure, for a quantitative measure of the lateral step relaxation the displacement of the atoms on the free step must be compared with the positions of the atoms of the second layer.

To estimate the strain on the step edge of an infinite island we performed calculations with island sizes varying between four and 48 atoms on a 50 atom wide cell. The barriers for approaching the case of an infinite island where then calculated on a 30 atom wide island on this slab.

The vicinal surfaces used for simulations of processes at kinks were (9,6,5) and (10,9,6), having kinked A- and B-steps respectively. The width of the terraces and the distance between the kinks are four atoms.

The calculations at the corners are interesting for comparison with vacancy islands as studied by Lundgren et al. [20]. If we had used a slab geometry with a complete vacancy island here, this would have either required a very big unit cell, or would have resulted in too small a vacancy island and thus would have introduced border effects. We rather used a cluster geometry with a rigid pot of atoms around the area of interest. This pot consisted of two-layer thick walls of atoms fixed in positions obtained by previous relaxation of appropriate slabs with periodic boundaries. The structure was 12×12 atoms wide and eight atoms thick, with a region of $8 \times 8 \times 6$ moveable atoms inside the pot (two uppermost layers shown in Fig. 2a). By that we minimized border effects on processes near the corner. An overview of the processes calculated on kinks and the concave corner can be seen in Fig. 2.

In addition to these calculations of energy barriers we did some molecular dynamics calculations at elevated temperature (60 meV, corresponding to 700 K) for a vacancy island as well as for vicinal surfaces. These simulations were done to find all relevant processes. An adatom was placed on the upper terrace and the kind of descent of the adatom into the vacancy island was checked. These calculations led us to include processes at starting points near the corners, where the adatom starts from hollow sites in "second row". These are the fcc sites on the A-step and the hcp sites on the B-step.

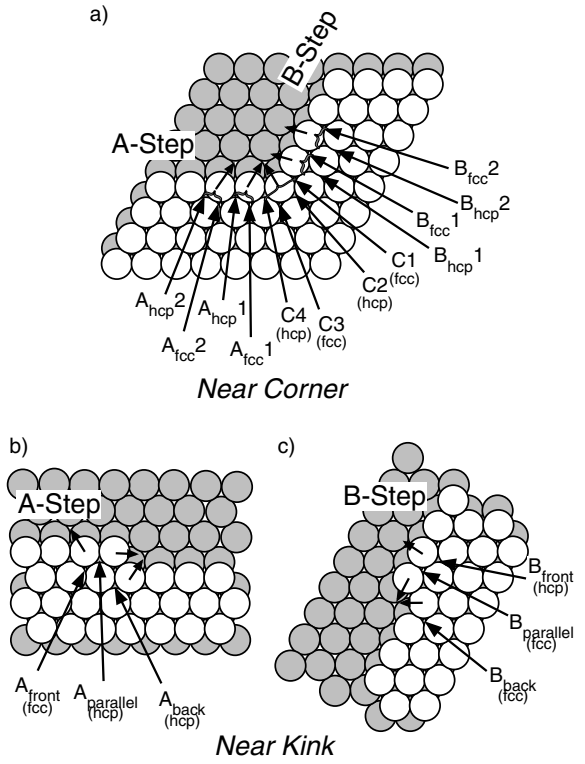

Fig. 2. Starting points of the adatoms for the calculated processes near kinks and the concave corner. The substrate atom undergoing the exchange and its direction of motion are indicated by small arrows. In the calculation, this atom is dragged out to the underlying surface (small arrows). In the processes $A_{parallel}$ and $B_{parallel}$ the kink atom is dragged away along the step edge.

3. Results and discussion

3.1. Steps

In Tables 1 and 2 we present the results obtained for the exchange and hopping processes on

Table 1
Activation barriers and Schwoebel barriers at straight steps calculated using (4,3,3) and (4,4,3) vicinal surfaces for A- and B-steps, respectively[a]

Step	Pt adatom			Ni adatom		
	Activation barrier	Schwoebel barrier	Starting energy	Activation barrier	Schwoebel barrier	Starting energy
A (from fcc)	0.29 (0.83)	0.20 (0.74)	−0.09	0.37 (0.65)	0.17 (0.44)	−0.20
A (from hcp)	0.28 (0.81)	0.20 (0.74)	−0.08	0.39 (0.67)	0.17 (0.44)	−0.23
B (from fcc)	0.17 (0.81)	0.08 (0.73)	−0.08	0.32 (0.67)	0.09 (0.44)	−0.23
B (from hcp)	0.19 (0.83)	0.08 (0.72)	−0.10	0.30 (0.65)	0.09 (0.44)	−0.21

[a] Values in parentheses are for hopping processes, starting energies are with respect to the transition state for diffusing on a flat terrace (see Fig. 1c). All values in eV.

Table 2
Activation barriers and Schwoebel barriers at straight steps of a four row wide stripe shaped island[a]

Step	Pt adatom			Ni adatom		
	Activation barrier	Schwoebel barrier	Starting energy	Activation barrier	Schwoebel barrier	Starting energy
A (from fcc)	0.36 (0.83)	0.27 (0.75)	−0.09	0.41 (0.64)	0.22 (0.45)	−0.19
A (from hcp)	0.34 (0.81)	0.27 (0.75)	−0.07	0.45 (0.67)	0.23 (0.45)	−0.22
B (from fcc)	0.19 (0.81)	0.12 (0.74)	−0.07	0.35 (0.67)	0.12 (0.45)	−0.22
B (from hcp)	0.21 (0.83)	0.12 (0.74)	−0.09	0.33 (0.65)	0.12 (0.44)	−0.21

[a] Values in parentheses are for hopping processes, starting energies are with respect to the transition state for diffusing on a flat terrace. All values in eV.

straight steps using vicinal surfaces and a stripe-shaped island, respectively. The results for the hopping process are written in parenthesis, they are significantly higher in every case so we claim hopping processes to be negligible against the exchange processes. The results for the processes on the vicinal surfaces are also shown in Fig. 3 as the leftmost and rightmost columns.

For both kinds of adatom, Pt and Ni, we get a smaller activation barrier and thus a lower Schwoebel barrier for the exchange process on the B-step than on the A-step. The results we obtained for Pt correspond very well to earlier calculations [5] with other EAM-potentials, but are in sharp contrast to ab initio calculations by Feibelman [2] using LDA, where the activation barrier on the B-step was found to be significantly higher (0.64 eV). The activation barriers for the A-step are comparable, however (0.29 versus 0.31 eV, Ref. [2]). Taking the ab initio results as a reference, the big discrepancy found for B steps might be seen as an indication for rather poor reliability of our calculations. It should be noted however, that the experimental study [21] initially taken as confirmation of the LDA results [2] indicates easy step descent for islands bounded by B-steps only. Later, it has been argued that the step edges were not straight in this case, so that the low Schwoebel barrier at B-steps can also be explained by a high kink density [16]. In this paper Kalff et al. also give a Schwoebel barrier of $\approx$0.2–0.25 eV for straight B-steps, but in this case the surface was covered with 90 ML Pt at a low deposition rate, conditions where it is almost impossible to exclude the influence of adsorbed CO. A lower exchange barrier at the B-step is also in agreement with ab initio calculations for Al/Al(1 1 1) [12] as well as with FIM data [7,8] for Ir(1 1 1), a metal very similar to Pt.

Feibelman explains his results by the coordination number of the adatom in the transition state, claiming that on the A-step the adatom is 4-fold coordinated, whereas on the B-step the coordination is only 3-fold. To compare the nearest neighbour distances for the two steps we have plotted them in a diagram (Fig. 4) for the transition state

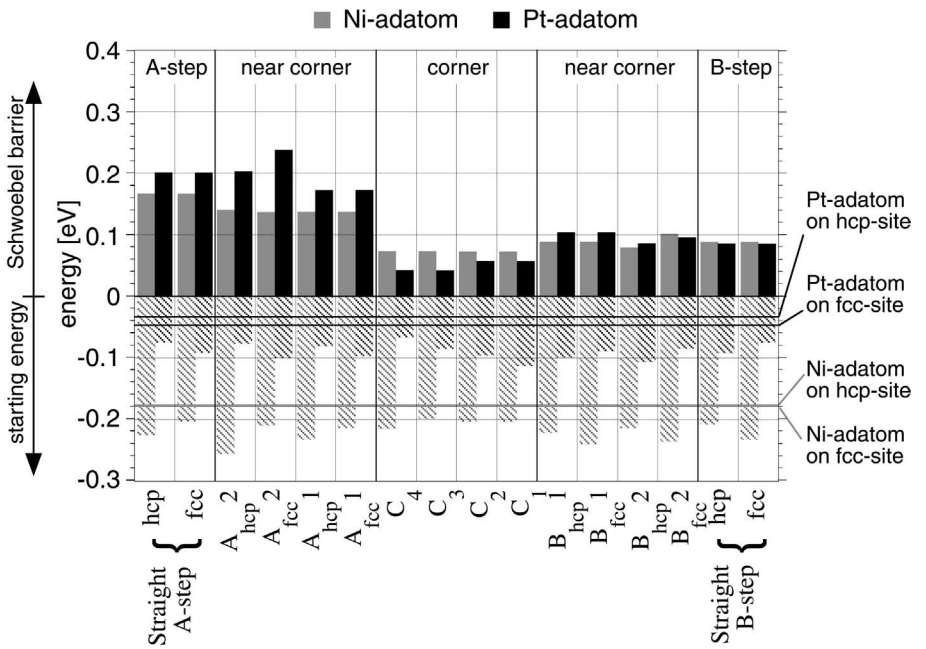

Fig. 3. Activation barriers and Schwoebel barriers of transitions near the corner. All energies are with respect to the transition state of diffusion over the plain Pt(1 1 1) surface. The black and grey full bars represent the Schwoebel barrier, whereas the black and grey hatched bars show the adsorption energy of the adatom in the starting position. Hence, the total length of the bars (full plus hatched) gives the activation barrier. The horizontal lines indicate the adsorption energy in fcc and hcp sites on the plain terrace (the hcp–fcc difference is only 20 meV for Ni adatoms). For comparison the barriers on the straight steps are given at the left and right end of the graph (vicinal (4,3,3) surface for A-step and (4,4,3) surface for B-step).

of the descent of a Pt adatom. In the transition state, the adatom on the A-step has four nearest neighbours in a distance of 2.45 Å (atom E in Fig. 4a), 2.46 Å (atom U_1), 2.65 Å (S_1) and 2.66 Å (U_2). On the B-step, we also find four neighbours roughly within the bulk next neighbour distance. In contrast to Ref. [2], the adatom in the transition state does not sit in a symmetric position corresponding to an hcp site, but is rather shifted along the step towards a fourfold hollow site, bringing it nearer to atom S_2 on the step edge (see Fig. 4b). However, this transition geometry was not allowed in the calculations of Feibelman, where the symmetric geometry was favoured. Atom S_2 has a distance of 2.78 Å from the adatom and can therefore still be considered a nearest neighbour, as the nearest neighbour distance in the bulk is 2.77 Å. To check the effect of the asymmetry of the transition state we also performed calculations enforcing a mirror plane through atoms A, E and L_2. This yields an increase of the barrier by 30 meV for the Pt adatom and 73 meV for the Ni adatom. This rather small effect does not explain the large difference to the barriers given in Ref. [2], however.

A larger difference between the two step geometries can be found by considering the distances of the neighbours to the atom pushed out of the step edge (atom E in Fig. 4). On the A-step we find only four atoms that we can consider nearest neighbours to this atom, and three more atoms somewhere between the first and second neighbour shell distance of the bulk, all further than 2.88 Å from atom E. This atom can therefore only be considered 4-fold coordinated. On the B-step, however, the atom pushed out is clearly 6-fold coordinated. As the binding energy is highly sensitive to the coordination, it becomes clear why the transition on the B-step is easier than on the A-step.

The comparison of the Schwoebel barriers for Pt and Ni adatoms shows nearly no difference on the

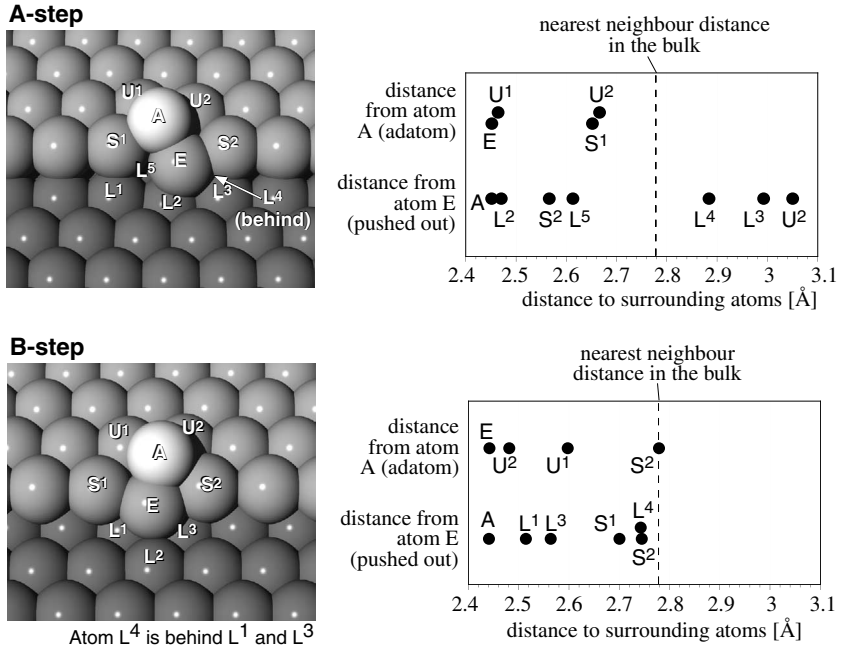

Fig. 4. Transition states at descent of a Pt adatom on straight steps. The right diagrams show the distance between adatom (atom A) or atom been pushed out of the step (atom E) and its nearest neighbours in the transition state. Each point stands for one of the atoms labelled in the corresponding left frame.

B-step, and only a 50 meV higher barrier for the Pt adatom on the A-step. The activation barriers are significantly larger for Ni than for Pt adatoms, however. As the Schwoebel barrier is the difference between activation barriers for step descent and for diffusion on the flat terrace, and both barriers are higher for Ni than for Pt, the difference between Pt and Ni almost cancels out when calculating the Schwoebel barrier. The same effect is also found for step descent at other sites (see below).

Comparing the Schwoebel barriers for descent from a stripe shaped island (Table 2) and descent on a vicinal surface (Table 1) one notices a significantly lower barrier (by up to 74 meV for Pt on the A-step) on the vicinal surface. At the first glance, this is quite astonishing, as one would expect easier relaxations of the atoms in the island (by moving atoms in the other step) lowering the barriers. We will show that the different barrier heights are rather due to different in-plane shifts of the step atoms in the two kinds of simulation cells.

As a measure of in-plane relaxation, a plot of the row-wise atom displacement versus the row number is given in Fig. 5. These displacements are due to tensile surface stress and cause different in-plane relaxation of the steps in the finite cells considered here. When comparing the row-wise displacement of the atoms in the stripe shaped island (filled circles) with the displacement on the vicinal surface (open circles), we find a larger displacement on the vicinal surface than on the island. This is due to the fact that the surface stress on the island can be reduced by movement of the atoms in the opposite step. By calculating the energy barriers for the descent on a step edge under tensile and compressive strain as described earlier, we can determine the influence of the in-plane relaxation on the barriers for the exchange processes (Fig. 6a and b). We find that inwards relaxation of the step edge due to tensile surface stress lowers the Schwoebel barrier the same way on both types of step edges and for both kinds of adatoms. Furthermore we find that the difference in energy

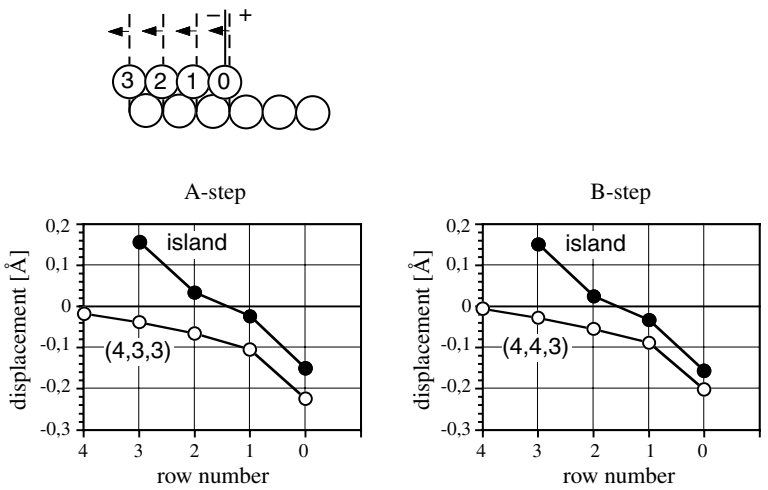

Fig. 5. In-plane relaxation of the atoms at steps of a stripe shaped island four atoms wide (●) and vicinal surfaces (○). For the sign of the displacement see the figure above. The displacement of the first layer atoms relative to their bulk positions is larger on the vicinal surface.

barriers of the exchange processes between the vicinal surfaces and the island geometry is just as large as one calculates by only taking into account the different magnitude of the displacement of the atoms in the first row (larger symbols in Fig. 6a and b). We attribute the small difference of the starting energy for the Ni adatom on the step edge under tensile strain to effects of the finite island size and the fixed atoms on the back side of the island.

A closer examination of the transition states of these processes shows that during descent the transition state is reached earlier, with the adatom still sitting higher over the first layer, when tensile strain is applied. After that the cohesive energy decreases as the adatom is pulled inwards. Therefore, we attribute the lowering of the activation barrier and therewith of the Schwoebel barrier with increasing tensile strain to a reduced repulsion by the first layer atoms (S_1, S_2, U_1, U_2 in Fig. 4). This softening of the close-packed surface with increasing tensile strain allows the adatom to sink into the terrace more easily. We consider the contribution of the atom pushed out (E in Fig. 4) to the lowering of the barrier less important, as it is close to a bridge site of the lower terrace in all configurations.

It should be mentioned, however, that surface stress is underestimated by EAM. For Pt(1 1 1), our EAM potentials give a surface stress of 1.39 eV/atom, ab initio calculations give between 2.20 eV/atom [37] with the GGA method and 2.49 eV/atom [37] or 2.61 eV/atom [38] with LDA (all calculations performing full relaxation of the atoms). As higher tensile surface stress will lead to an even larger in-plane relaxation of the step edge, one should expect a further lowering of the Schwoebel barriers for all processes we investigated. This is of particular importance for exchange processes on the B-step, as the barrier is already rather small, but it is even more important for barriers on more complex sites like kinks and corners, as there the barriers we found are even smaller (see Section 3.2).

3.2. Kinks

The Schwoebel barrier for descent near to or at kinks largely depends on the kind of step edge the kink is at (Fig. 7). On the A-step the barrier is quite high for the process where the adatom descends on the outer side of the kink (process A_{front}, see Fig. 2), but very low – even negative – directly at the kink (process A_{back}), in agreement with

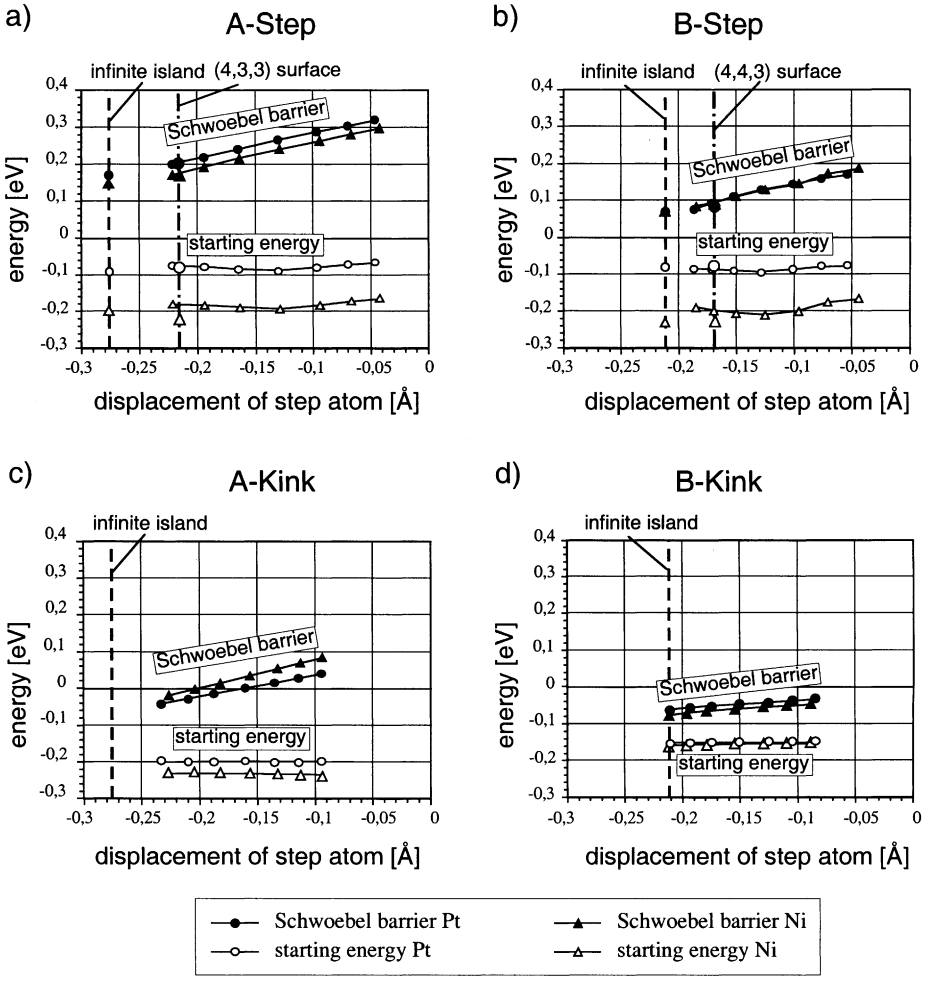

Fig. 6. Activation barriers and Schwoebel barriers of transitions under strain causing in-plane displacement of the step atoms. As in Fig. 3, the energy difference between the upper (Schwoebel barrier) and the lower point (starting energy) for each case gives the transition barrier. Large symbols represent points calculated for vicinal surfaces.

Ref. [5]. Negative Schwoebel barriers have been reported for the very open ⟨1 0 0⟩ steps of Ag(0 0 1) [39]. Our results indicate that they are also possible for special sites of close packed surfaces. Although process A_{back} itself is similar to descent at the corner (in particular to process C2, see Fig. 2 and Section 3.3), the barrier is much lower at the kink. This results from a larger inwards relaxation of the kink atom, which brings it closer to the exchanged atom to compensate for the loss of bonds of the exchanged atom to the atoms in the upper terrace behind it. In the case of the corner this relaxation is hindered by the attraction of the neighbouring atom along the B-step. The higher barrier for the process A_{front} results from an increasing distance between the kink atom and the exchanged atom. In contrast to the similar process B_{front} the kink atom at the A step cannot relax towards the exchanged atom, as its way is blocked by the underlying atom in the lower terrace between them.

On the B-step the result is quite the opposite. Descent on the outer side of the kink (process B_{front}) has the lowest barrier of all calculated processes for both types of adatom. For the Pt adatom,

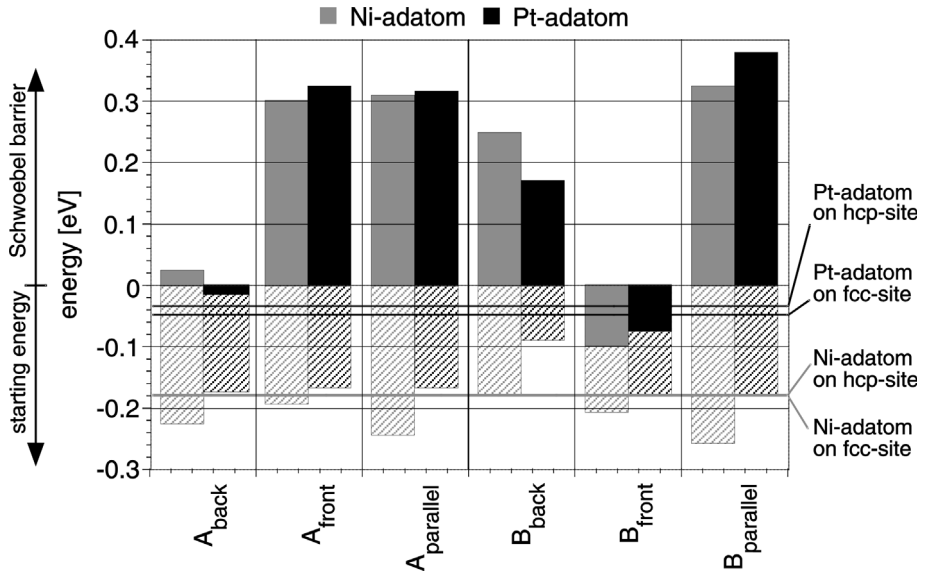

Fig. 7. Activation barriers and Schwoebel barriers of transitions near the kinks of the vicinal surfaces described in the text. The bars represent the same values as in Fig. 3. The adsorption energies of the adatoms on the plain surface are sketched as lines again. Note that there are also negative Schwoebel barriers. The activation barriers are the full length of the bars (hatched plus filled bars) for positive Schwoebel barriers, and the length of the hatched bar only for negative Schwoebel barriers.

the energy in the transition state is even lower than the adsorption energy on a flat terrace. This process is very similar to step descent on the straight B-step, only that the step edge ends after the atom S_2 (Fig. 4). Thereby this atom is less constrained to move parallel to the step edge and moves towards the atom dragged out of the step. This freedom to move explains the large reduction of the activation barrier for this process. On the other hand, for the process directly in the corner (process B_{back}, see Fig. 2) the barrier is higher than the barrier in the geometrically similar process with a corner geometry (Section 3.3) and higher than the exchange process on a straight B-step, again in agreement with Ref. [5]. The exchanged corner atom is pushed out of the step edge through the bridge position between the underlying surface atoms. Thereby the distance to its neighbouring atom in the step is increased. This neighbouring atom follows the exchanged atom and looses the bond to the next atom in the step edge, but it is still too far from the adatom to bind to it. The adatom remains 3-fold coordinated and the exchanged atom is only 5-fold coordinated. Therefore the process has a rather high Schwoebel barrier. These results are the same for the calculations using an island geometry and for the calculations using vicinal surfaces.

The high barriers of the processes $A_{parallel}$ and $B_{parallel}$, where the kink atom has to move along the step edge to make space for the adatom can only partly be explained by the barrier of the atom diffusing along the step. According to EMT calculations [6] the diffusion of adatoms along the B-step has a barrier only slightly above the diffusion over the flat surface (0.18 eV compared to 0.16 eV), and the barrier for the atom diffusing along the A-step is higher than for diffusion along the B-step (0.23 eV). This tendency also results from ab initio calculations [40] (0.71 eV for the A-step, 0.77 eV for the B-step), although the energies are far above the barrier for adatom self-diffusion on Pt(1 1 1) (0.29 eV according to Ref. [40]). In our case, process $B_{parallel}$ has a higher barrier than $A_{parallel}$, and both barriers are well above that for diffusion along the flat surface. We therefore conclude that the main influence to these barriers is the breaking of the bond to the neighbouring step atom at the front side of the kink.

Again, we applied artificial strain to the island geometry as we had done with the straight step, and checked the influence of strain on the Schwoebel barrier of the exchange processes A_{back} and B_{back} (Fig. 6c and d). We found similar results as on the straight step.

The activation barriers for most processes near the kink are nearly independent of the kind of adatom we use, which is in contrast to the results obtained on the straight steps. This also supports our conclusion, that here the main contributions to the barrier come from the atom which is dragged out from the corner and the kink atom itself, whereas the adatom seems to have only little effect.

3.3. Corners

In Fig. 3 we present the results of our calculations for descent of the adatom near to or at a corner. In comparison to the barriers for descent at straight steps (left and right side of Fig. 3), one notices that the activation barrier gets smaller, when the process takes place at the corner.

As on the straight steps, near the corner we find a large difference in the barriers between descent on A-steps and descent on B-steps, the exchange process at the B-steps requiring less energy and therefore being more likely to happen. Near the corners we again notice a difference between the Schwoebel barriers of the two kinds of adatom, where the difference in barrier between the two kinds of adatom is larger on the A-step than on the B-step. Directly at the corner the energy barriers for the Ni adatom are the same for almost all starting points. The reason is that from all starting points except for C1 the Ni adatom first moves around the underlying corner atom reaching a 4-fold hollow site between the points C2 and C3 in Fig. 2 when the corner atom has moved out a little. From that point, all processes continue the same way yielding the same Schwoebel barrier. From the starting point C1 the adatom reaches a position between C1 and C2 before descending. The Pt adatom does not move that far but rather stays near its initial position. For the starting points C1 and C2 this means that the adatom reaches the same transition state between the two starting positions. This is somewhat unexpected, as Ni has a higher diffusion barrier on the plain surface than Pt. One therefore would rather expect the Pt atom to move around the corner atom.

As the corner atom is pushed onto the terrace, the transition states themselves are quite similar to the processes A_{back} and B_{back} at the kinks. At the first glance, one might consider it difficult to push the corner atom through the narrow space between the two adjacent step atoms, but the opposite is true: similar to the (tensile) surface stress of metals, the low coordination of the step edges causes an even stronger tensile stress in the steps. In the corner the step atoms adjacent to the corner atom therefore are hindered to relax towards the corner. This results in a higher Schwoebel barrier than in the case of A_{back}, as the corner atom loses bonds to the atoms behind it in the upper terrace without getting compensation for this by a sufficiently shorter bond length to its neighbour along the B-step (the atom corresponding to the kink atom of an A-step kink). The tensile force along the step edges also explains the lowering of the Schwoebel barrier with respect to the process B_{back}. There as well as in the corner processes the atom adjacent to the exchanged atom along the A-step – which corresponds to the kink atom on the B-step – does not relax inward to the exchanged atom, but the reason for this is slightly different. While in process B_{back} the only reason for the kink atom not to relax inwards is the blocking atom in the underlying terrace (see Section 3.2), in the corner process there is an additional tensile force on this atom from its neighbour along the step edge. This force prevents the atom from relaxing towards the corner.

4. Conclusion

We have presented energy barrier calculations for a large set of hopping and exchange processes of Pt and Ni adatoms descending steps on the Pt(1 1 1) surface. For the processes previously studied by Villarba and Jónsson, we obtain results similar to their study [5]. We also find that the results for Ni adatoms are generally similar to those of Pt self-diffusion. We further argue that the results for Ni should be representative for the recently studied Co/Pt(1 1 1) system as well.

From the comparison of the barrier heights we have shown that for the down-step movement of adatoms exchange processes are energetically favoured to hopping processes in every case. We have also shown that descent on the B-step is favourable as compared to the similar process on the A-step, and we have shown that this energetic advantage is due to the higher coordination number of the exchanged atom on the B-step. These results are in agreement with experimental findings [7,8], but in contrast to a recent ab initio study [2].

We have further shown that for concerted substitution processes atomic configurations with lower symmetry such as concave corners and kinks are preferred places, as there all atoms involved in the process can keep a high coordination, or in case of the exchanged atom, at least compensate for their loss of coordination by a tighter binding to another atom. This is especially true for kinks, where even negative Schwoebel barriers are found. This supports the proposed model for reentrant layer-by-layer growth of Pt(1 1 1) [15,6], where 2D growth in the low temperature regime is due to the high kink density, whereas in the medium temperature regime, where kinks are smoothed out, atoms on the upper terrace cannot descend that easily any more. This also corresponds to the findings of the Co adsorption experiment [20], which shows that almost all the corners are occupied by Co atoms sitting behind Pt atoms indicating that corners are favourable places for descent of adatoms. Actually the only places where the energy barrier for the descent is even lower are kinks. Although not all details are clear yet [41] in the images published in Ref. [20] one also notices Co adatoms behind the kinks.

Another very important result is the effect that surface strain has on the energy barriers. We find that in-plane relaxation of the step atoms caused by the tensile surface stress of Pt(1 1 1) lowers the Schwoebel barrier on both A- and B-steps, independent of the kind of adatom. This also has consequences for the barriers obtained by other semi-empirical studies as well as ab initio calculations, as the models used in energy calculations are often too small to obtain a fully relaxed step edge. In addition, the influence of step relaxation must be also considered when discussing the results of FIM measurements, as island sizes are very limited in these experiments, too.

Acknowledgements

Support by the Fonds zur Förderung der wissenschaftlichen Forschung (START-program Y75) and the TMR programme of the EU (Marie Curie Research Training Grants) is gratefully acknowledged.

References

[1] E. Chason, B.W. Dodson, J. Vac. Sci. Technol. A 9 (1991) 1545.
[2] P.J. Feibelman, Phys. Rev. Lett. 81 (1998) 168.
[3] K. Kyuno, G. Ehrlich, Phys. Rev. Lett. 81 (1998) 5592.
[4] P.J. Feibelman, J.S. Nelson, G.L. Kellog, Phys. Rev. B 49 (1994) 10548.
[5] M. Villarba, H. Jónsson, Surf. Sci. 317 (1994) 15.
[6] J. Jacobsen, K.W. Jacobsen, P. Stoltze, J.K. Nørskov, Phys. Rev. Lett. 74 (1995) 2295.
[7] S.C. Wang, G. Ehrlich, Phys. Rev. Lett. 67 (1991) 2509.
[8] S.C. Wang, G. Ehrlich, Phys. Rev. Lett. 75 (1995) 2964.
[9] S.C. Wang, T.T. Tsong, Surf. Sci. 121 (1982) 85.
[10] K. Kyuno, A. Gölzhäuser, G. Ehrlich, Surf. Sci. 397 (1998) 191.
[11] M. Bott, M. Hohage, M. Morgenstern, Th. Michely, G. Comsa, Phys. Rev. Lett. 76 (1996) 1304.
[12] R. Stumpf, M. Scheffler, Phys. Rev. Lett. 72 (1994) 254.
[13] R. Stumpf, M. Scheffler, Phys. Rev. B 53 (1996) 4958.
[14] M. Bott, Th. Michely, G. Comsa, Surf. Sci. 272 (1992) 161.
[15] R. Kunkel, B. Poelsema, L.K. Verheij, G. Comsa, Phys. Rev. Lett. 65 (1990) 733.
[16] M. Kalff, P. Smilauer, G. Comsa, Th. Michely, Surf. Sci. 426 (1999) L447.
[17] J.A. Meyer, J. Vrijmoeth, H.A. van der Vegt, E. Vlieg, R.J. Behm, Phys. Rev. B 51 (1995) 14790.
[18] Y. Suzuki, H. Kikuchi, N. Koshizuka, Jpn. J. Appl. Phys. 27 (1988) L1175.
[19] H.A. van der Vegt, H.M. van Pinxteren, M. Lohmeier, E. Vlieg, J.M.C. Thornton, Phys. Rev. Lett. 68 (1992) 3335.
[20] E. Lundgren, B. Stanka, G. Leonardelli, M. Schmid, P. Varga, Phys. Rev. Lett. 82 (1999) 5068.
[21] M. Kalff, G. Comsa, Th. Michely, Phys. Rev. Lett. 81 (1998) 1255.
[22] G. Ritz, M. Schmid, A. Biedermann, P. Varga, Phys. Rev. B 53 (1996) 16019.
[23] W. Hebenstreit, G. Ritz, M. Schmid, A. Biedermann, P. Varga, Surf. Sci. 388 (1997) 150.
[24] Y. Gauthier, R. Baudoing-Savois, J.M. Bugnard, Surf. Sci. 276 (1992) 1.

[25] Y. Gauthier, P. Dolle, R. Baudoing-Savois, W. Hebenstreit, E. Platzgummer, M. Schmid, P. Varga, Surf. Sci. 396 (1988) 137.
[26] Y. Gauthier, R. Baudoing-Savois, J.J.W.M. Rosink, M. Sotto, Surf. Sci. 297 (1993) 193.
[27] J.M. Bugnard, R. Baudoing-Savois, Y. Gauthier, E.K. Hill, Surf. Sci. 281 (1993) 62.
[28] P. Weigand, B. Jelinek, W. Hofer, P. Varga, Surf. Sci. 307–309 (1994) 416.
[29] P. Weigand, B. Jelinek, W. Hofer, P. Varga, Surf. Sci. 295 (1993) 57.
[30] L.Z. Mezey, W. Hofer, Surf. Sci. 352 (1996) 15.
[31] L.Z. Mezey, W. Hofer, Surf. Sci. 331 (1995) 799.
[32] M. Methfessel, D. Hennig, M. Scheffler, Appl. Phys. A 55 (1992) 442.
[33] P. Stoltze, Simulation Methods in Atomic-scale Material Physics, Polyteknisk Forlag, Lyngby, 1997.
[34] H. Jónsson, G. Mills, K.W. Jacobsen, in: B.J. Berne, G. Ciccotti, D.F. Coker (Eds.)., Classical and Quantum Dynamics in Condensed Phase Simulations, World Scientific, Singapore, 1998, p. 385.
[35] G. Ehrlich, F.G. Hudda, J. Chem. Phys. 44 (1966) 1039.
[36] R.L. Schwoebel, E.J. Shipsey, J. Appl. Phys. 37 (1966) 3682.
[37] G. Boisvert, L.J. Lewis, Phys. Rev. B 57 (1998) 1881.
[38] P.J. Feibelman, Phys. Rev. B 56 (1997) 2175.
[39] U. Kürpick, T.S. Rahman, Phys. Rev. B 57 (1998) 2482.
[40] P.J. Feibelman, Phys. Rev. B 60 (1999) 4972.
[41] M. Schmid, E. Lundgren, G. Leonardelli, A. Hammerschmid, B. Stanka, P. Varga, Appl. Phys. A 72 (2001) 405.